DOI: 10.1021/ma100112g

Macromolecules
ARTICLE

Enzyme Entrapment in Reprecipitated Polyaniline Nano- and Microparticles

Louis R. Nemzer,[†] Austin Schwartz,[†] and A. J. Epstein*[,†,‡]

[†]*Department of Physics, The Ohio State University, Columbus, Ohio 43210-1117, and*
[‡]*Department of Chemistry, The Ohio State University, Columbus, Ohio 43210-1173*

Received January 20, 2010; Revised Manuscript Received April 2, 2010

ABSTRACT: We introduce a novel method for fabricating nano- and microscale polyaniline particles containing an entrapped oxidoreductase enzyme for use in biosensing applications. This facile process utilizes the reprecipitation of the emeraldine base form of polyaniline from an aqueous−organic suspension, with hydrophobic collapse and subsequent cross-linking of the polymer induced by adjusting the ionic strength beyond a critical threshold. We present UV−vis spectroscopy data, including a quantitative treatment of the spectral line width, along with dynamic light scatting results, to explain the conformation changes in the polyaniline chains that accompany this transition. The resultant aggregated supermolecular polyaniline formations immobilize enzymes via gelation entrapment, augmented by electrostatic attraction, without the need for harsh reaction conditions or additional reagents. Because of its strong optical features at visible wavelengths that can serve as probes for chain conformation, oxidation state, and protonation level, polyaniline may act as a model system for the study of hydrophobic and ion screening effects in proteins and other foldamers.

Introduction

A biosensor is a device that implements a sensing element to transduce a particular biological property into a signal[1] that can be ultimately converted into machine-readable data. Modern medicine is increasingly reliant on information from such sensors to facilitate a timely diagnosis and to direct the course of treatment. Because of the high specificity and catalytic activity of enzymes, methods that immobilize these proteins present great value in the effort to fabricate multiuse and continuous-use biosensors. Additionally, entrapment may enhance the stability of enzymes by constraining them to maintain a native conformation[2] while still permitting the motions required for normal binding and chemical activity,[3] and remaining permeable to analyte diffusion.[4] Organic polymers, including polyaniline, have been made to immobilize enzymes during initial synthesis via electrochemical polymerization,[5] or afterward using covalent bonding,[6] for example, by graft copolymerization.[7] These methods have a potential advantage in that leakage may be minimized, leading to higher stability.[8] However, covalent attachment requires several chemical steps, and electrochemical polymerization exposes the enzymes to harsh, often strongly acidic,[9] conditions, potentially with denaturing effects. Thus, the development of new biosensors depends on simple and robust immobilization methods.[3] In this work, we introduce a novel reprecipitation[10] method using noncovalent supermolecular cross-linking,[11] suitable for a wide variety of nanostructure fabrication uses, and with the ability to achieve concomitant immobilization of desired macromolecules, such as oxidoreductase enzymes, under much more amenable reaction conditions.

Polyaniline, an intrinsically conducting organic polymer, has proven to be biocompatible,[12] easily processed,[13] and rapidly converted between electrically insulating and conductive forms. Emeraldine base (EB), the half-oxidized form of undoped polyaniline, consists of half amine and half imine repeat units (Figure 1). Exposure to a protic acid,[14] such as HCl, dopes the nonconductive EB to create emeraldine salt (ES). The ES form exhibits a polyionic structure, which may also be obtained through "pseudodoping" with ionic salts.[15] Polyaniline has attracted a great deal of attention for its ability to couple with oxidoreductase enzymes and, consequently, its utility as part of novel biosensors.[16] The capability for direct electron transfer[17] from the enzyme to the polymer has been demonstrated, highlighting the possibility of "solid state"[18] multiuse biosensors that do not require a mediating redox species.[19]

The facile and inexpensive nanoparticle synthesis and enzyme entrapment method introduced in this study does not require special reagents or material preparation. It makes use of the extremely limited solubility of EB in aqueous environments. This insolubility[20] extends even to most organic solvents.[21] Indeed, under ordinary conditions, the polymer will not form a true solution at all; rather, it can only be suspended in select polar aprotic organic solvents. Most of these solvents contain at least one amide group, in which the C=O group, with its resonance-stabilized dipole moment, can accept a hydrogen bond from an amine nitrogen in EB.[22] These include *N*-methyl-2-pyrrolidone (NMP), dimethylformamide (DMF), *N*,*N*,*N*′,*N*′-tetramethylurea (TMU), and *N*,*N*′-dimethylpropyleneurea (DMPU). Other solvents, such as tetrahydrofuran (THF), dimethyl sulfoxide (DMSO),[23] and *m*-cresol, possess no amides but still have large dipole moments and nucleophilic oxygens. Thick EB films have previously been prepared from concentrated preparations (1−5% w/w) of emeraldine base in NMP via gelation by physical cross-linking,[24] in which, upon removal of the solvent, imine nitrogens instead form hydrogen bonds with the secondary amines of neighboring chains[25] (Figure 2).

More dilute suspensions can be drop-cast or spin-coated onto glass slides, and will form thin films upon removal of the solvent by drying under dynamic vacuum and/or heat. Because of the large dipole moments of the solvents listed above, they are

*To whom correspondence should be addressed. E-mail: epstein@mps.ohio-state.edu.

 Published on Web 04/19/2010

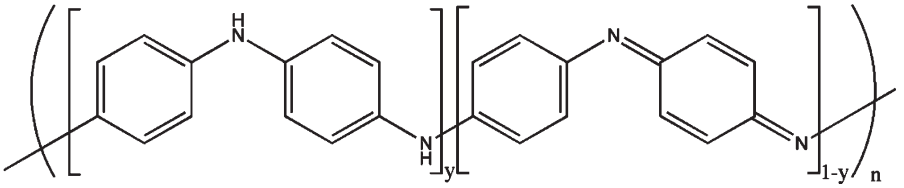

Figure 1. Basic polyaniline chemical structure. The index *y* denotes the proportion of chain repeat units in the reduced amine form, as opposed to the oxidized imine state.

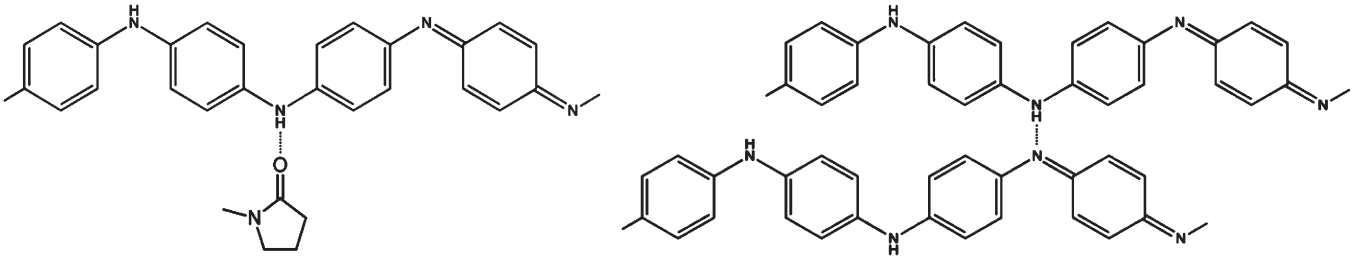

Figure 2. Hydrogen bonding between an amine group of an EB chain with (left) a solvating NMP molecule and (right) the imine group on an adjacent chain, creating a noncovalent cross-link.

miscible with water. Thus, if a small amount of a polymer suspension comprising one of the above "good solvents"[26] is added to a relatively large amount of an aqueous solution, a much poorer environment for PANI, the majority of the organic solvent will diffuse throughout the newly created binary solution, exposing the polymer chains to a predominately poor solvent microenvironment. However, the expected chain collapse and aggregation does not occur immediately. Because of the strong hydrogen bonding between the imine groups and their adjacent "good solvent" molecules, they do not diffuse into the bulk but remain coordinated to the polymer chain. The result is a colloidal system extremely sensitive to disruption by even trace amounts of ionic cosolutes,[27] which can interfere with this solvation arrangement. In addition, anions can polarize the amine N−H bonds in EB, reducing their ability to donate hydrogen bonds to the solvent molecules. After a critical ionic strength is reached, the solvent molecules will be displaced, and the strongly hydrophobic nature of polyaniline will cause it to collapse from an extended coil to compact coil conformation.[28] Depending on the final solvent environment, the polymer coils may further reduce their exposed area by aggregating, with hydrogen bond cross-linking, into microscale particles. In ES, the alteration in physical properties, such as conductivity and electronic structure, that accompany a transition from extended to coiled conformation has been studied under the rubric of "secondary doping",[29] defined as a change caused by a normally inert substance, with the effect persisting even after the material is removed. These changes are associated with the increased conjugation length that accompanies an extended chain conformation.

In the undoped EB form, an extended conjugation length has been correlated with a red-shifting and broadening of the main exciton absorption peak near 630 nm, in which a valence electron from an orbital centered on an amine repeat unit is excited to the LUMO level centered on an adjacent imine repeat unit.[30] Bathochromic shifts of this optical feature have also been observed and have been similarly attributed[31] to a conformation change from a tightly coiled to an expanded-coil shape in good solvents, such as NMP. Additional solvatochromatic relationships in polyaniline derivatives[31] were noted involving solvents with high donor numbers, which indicates basicity and thus ability of solvate cations. Since these solvents can help stabilize the positive centers of the excited state, as well as accept hydrogen bonds, the spectra were red-shifted compared with those involving solvents of lower donor number. In this way, knowledge of the intensity, peak wavelength,[32] and line shape of the molecular exciton absorption feature is a sensitive probe of the polymer's conformation, which, in turn, is strongly influenced by its immediate environment.

Experimental Section

Stock Solutions. Polyaniline was synthesized by oxidative polymerization as described elsewhere.[33] The product was stirred with dilute NH_4OH for ~12 h to ensure complete deprotonation. It was then filtered, washed with methanol and then deionized (DI) water, and dried under dynamic vacuum. A stock solution of EB in NMP with nominal concentration of 6 mg/mL (~0.6% w/w) was passed through a 0.45 μm syringe filter followed by a 0.2 μm filter. A THF stock was prepared similarly but did not require filtering beyond 0.45 μm. A "half concentration" stock of EB in NMP was subsequently obtained by diluting the full concentration suspension 1:1 with addition solvent. The order is significant because many conjugated polymers exhibit "memory effects",[34] in which the final conformation state is affected by the solvents and concentrations[35] of suspensions the polymer previously inhabited.

Phosphate Buffered Saline. Phosphate buffered saline (PBS; 0.1 M, pH 7.4) is formulated with NaCl (137 mM), KCl (2.7 mM), Na_2HPO_4 (10 mM), and KH_2PO_4 (2 mM) and serves two crucial functions in this process. First, it is the preferred isotonic environment for dissolving enzymes. Second, the ionic salts induce the polymer collapse and gelation that ultimately entraps the enzyme. As part of this process, the cations in PBS cause the PANI to become positively charged, which holds the negatively charged enzymes via electrostatic attraction. The negative counterions screen these charges and help induce, and then stabilize, the collapsed state. As a divalent counterion, HPO_4^{2-} can also foster chain aggregation by forming bridges between positively charged chain sites.[36]

Nanoparticle Synthesis. For each sample, 0.1 mL of stock solution was diluted 1:9 to a final volume of 1 mL with DI water. Measured amounts of PBS diluted 100 times, to a concentration of 1 mM, were added. In the case of tetrahydrofuran samples, undiluted PBS was used. Visible particle precipitation occurred at definite salt concentrations for the NMP samples. The particle and supernatant fractions were separated by centrifuging at 5500 rpm for 30 min and then allowing to settle overnight. DI water was added to level the total volume of all samples at 1.4 mL. After removal of a 1 mL aliquot of the supernatant, the particles were resuspended in the remaining liquid with a vortexer (Fisher Scientific Variable Speed Analog #02-215-365).

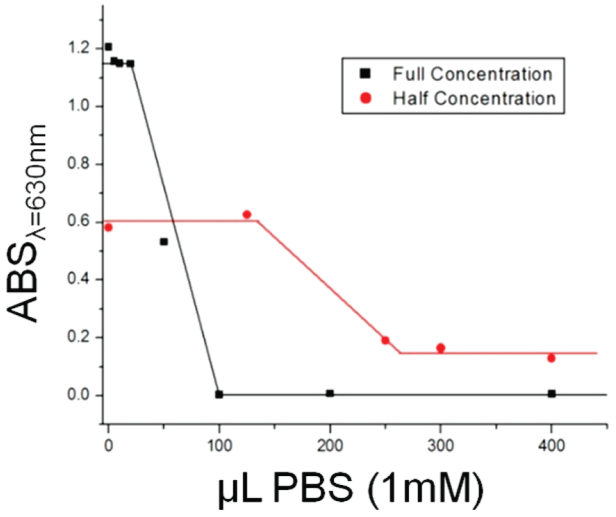

Figure 3. Optical absorption at 630 nm for the NMP supernatant samples described in the text. After hydrophobic collapse, virtually all the polyaniline is in the form of particles, leaving the supernatant almost clear. The lines are guides for the eye.

UV−vis Spectroscopy. As the concentration of PBS was increased, a greater fraction of EB from the NMP suspensions aggregated to form particles. This transition is discontinuous; at a critical threshold the sample goes from a uniform light blue liquid to a suspension of reprecipitated particles dispersed in a clear supernatant (Figure 3). Much less visible precipitation occurred in the THF samples, even after undiluted PBS was added.

This can be understood in light of the fact that THF can only suspend EB oligomers, so there is much less material present for particle formation, and the limited size of the chains prevented cross-linking.

There are several important features to note in the transition experienced by the NMP solutions. While both the full- and half-concentration samples experienced a discontinuous change from a uniform blue suspension at low PBS to combination of particles and supernatant at higher salt concentrations, it took less PBS to precipitate the higher concentration of EB, as it was closer to the solubility limit. Also, its transition was sharper, since nucleation of some particles increases the likelihood that other polymer chains will do likewise. Similarly, the final yield of particles was more complete with the full concentration, where virtually all of the polyaniline participated in forming particles. More detailed information can be gleaned by plotting the peak wavelength and line width (Figure 4) of the exciton transition near 630 nm, which also demonstrated an abrupt regime change. ORIGIN data analysis software with a Lorentzian function was used to quantify the full width at half-maximum of the peaks; Gaussian and Voigt models yielded similar fits. In samples with salt concentrations below the critical threshold, the exciton peak shows a slight blue shift but demonstrated little change in line width. Once particle formation begins, both the precipitated particles and the supernatant showed a marked red shift and peak broadening. Although visible particles did not form for the THF samples, a phase transition was evident as well, but at a much higher salt concentration. Although, as with the NMP sample, the peaks were red-shifted with increasing ionic strengths, in THF the line widths showed a distinct narrowing beyond the critical threshold.

Scanning Electron Microscopy. After centrifuging, the particles were separated via decantation and dried under dynamic vacuum for SEM imaging. Charging effects were minimized by doping the EB to the conductive ES form with a very brief exposure to HCl vapor and using an ITO-coated glass substrate. The literature indicates that this doping does not have a significant change on the morphology.[37] By affixing a wire between the ITO surface and the SEM stud, a conduction path was provided for excess electrons to leave to ground. In the absence of the ionic salts, the polymer chains in the binary solution remain separate. Thus, when the cosolvents were evaporated away, a continuous, but highly structured film, results (not shown). In contrast, the nanoparticles precipitated by PBS have diameters as small as 60 nm (Figure 5a). Larger particles were obtained when an enzyme was immobilized inside, in this case, glucose oxidase (GOx) (EC 1.1.3.4), with 7.2 mg of GOx entrapped in 50 μL of EB (Figure 5b).

Dynamic Light Scattering. Polyaniline made polyionic by doping with camphorsulfonic acid (PANI-CSA) has been studied by Gettinger et al.[38] to quantify the effect of environment on the chain conformation. As the solvent was made increasingly worse using water, they found single extended chains with an effective hydrodynamic radius (R_H) of 45 nm coil into globules with a corresponding value as small as 17 nm. With a Brookhaven Instruments BI-200 SM goniometer DLS particle size analyzer (Figure 6), we have similarly found that in DI water the PANI-EB chains in the "half-concentration" sample remain primarily in the extended conformation, although some had collapsed. The peak for the extended states (Gaussian center R_H = 47.5 nm) had a total area about 83 times larger than the coiled states (Gaussian center R_H = 13.4 nm). Some aggregation was observed when urea (40 mM), a poorer solvent than NMP, was added to full-concentration sample, manifesting as a log-normal distribution (peak R_H = 113 nm), characteristic of many polymer coils clustering into larger, cross-linked supermolecules. With the minimum amount of PBS required to form visible particles (0.5 mM), complete coagulation was observed. The peak particle radius measured this way was ~1.5 μm.

Analyte Sensing Using Nanoparticles. As a demonstration of the effectiveness of the enzyme entrapment, an optical biosensor was constructed using agglomerated PANI microparticles entrained with GOx fabricated with this method. The particles were precipitated using the minimum concentration of PBS required to form visible particles (0.5 mM) in the presence of 1.7 units of GOx (from *Aspergillus niger*, 5800 units/g), then washed extensively with DI water to remove free enzyme, centrifuged, and then dried under dynamic vacuum on a transparent microscope slide. The slide was placed into a spectrophotometer cuvette with additional PBS to equilibrate for several hours. A Varian Cary 5000 UV−vis−NIR spectrophotometer was used to determine the peak absorption wavelength, which was found to be 610 nm. This absorption value was observed over time as aliquots of a glucose test solution were added, which had been previously allowed to mutarotate for at least 1 h prior to use in order to equilibrate between the α- and β-anomers.

In the wild, GOx catalyzes the oxidation of β-D-glucose to D-glucono-1,5-lactone with dioxygen as the electron and proton acceptor, creating hydrogen peroxide (H_2O_2) as a product. The D-glucono-1,5-lactone then spontaneously hydrolyzes to gluconic acid (D-gluconate) as represented in the reactions:[39]

$$\beta\text{-D-glucose} + O_2 \xrightarrow{\text{GOx}} \text{D-glucono-1, 5-lactone} + H_2O_2$$

$$\text{D-glucono-1, 5-lactone} + OH^- \rightarrow \text{gluconic acid}$$

In the present system, when GOx is immobilized in the polyaniline matrix, the polymer itself acts as the electron and proton recipient in the first reaction step instead of oxygen:[6]

$$\beta\text{-D-glucose} + \text{oxidized PANI repeat (imine)} \xrightarrow{\text{GOx}} \text{reduced PANI repeat (amine)} + \text{D-glucono-1, 5-lactone}$$

Thus, for each glucose molecule, there is a reduction of the half-oxidized EB one step toward the completely reduced form

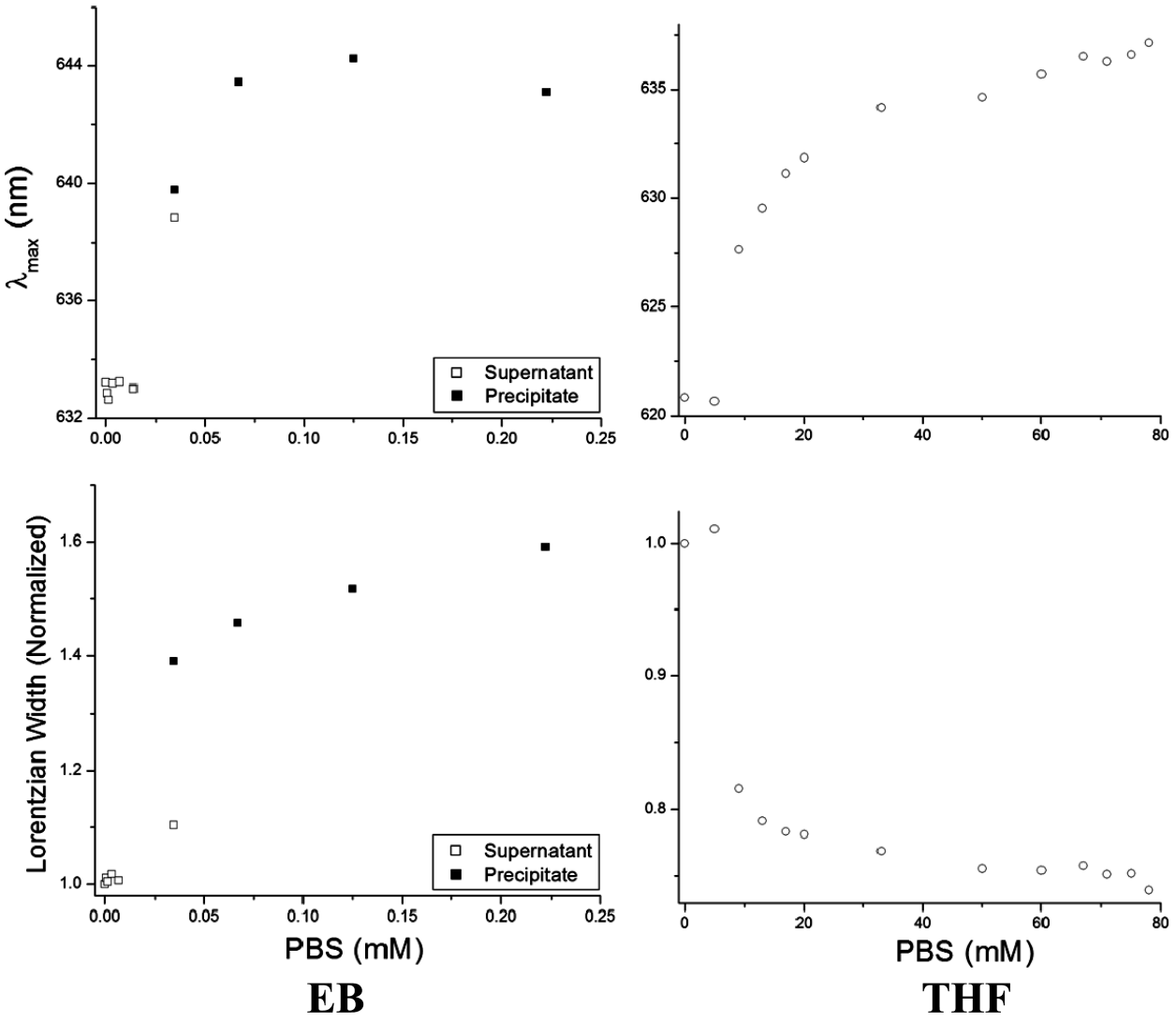

Figure 4. Peak exciton wavelength and normalized FWHM line width using a Lorentzian fit for EB in NMP/DI (full concentration) and THF/DI. The broadening and red-shifting of the exciton peak beyond the critical threshold for particle formation indicates a conformation change. Filled-in data points indicate particle samples, while open shapes are supernatants. For comparison, EB in pure NMP has a peak near 627 nm.

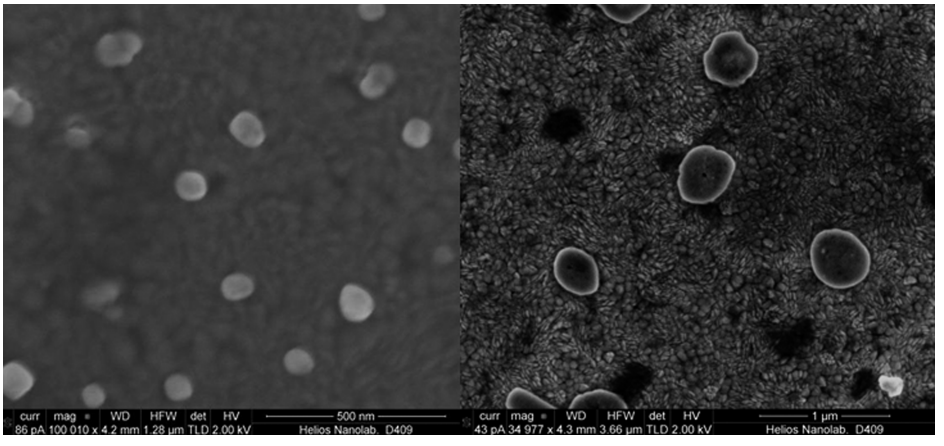

Figure 5. Scanning electron micrograph of EB nanoparticles on an ITO substrate without (left) and with (right) GOx cast from a binary solution of NMP with PBS.

when one imine repeat unit accepts two protons and two electrons from a glucose molecule to create an amine unit. Since the imine repeat is an intrinsic part of the chromophore that experiences the exciton transition, the intensity of the absorption will be suppressed as the population of imines is depleted by this process. Under physiological conditions, the EB form is most stable, and the reduced form will be quickly reoxidized by dissolved oxygen or other ambient species, so the polymer can regenerate on an ongoing basis. This is significant because previous efforts to fabricate polyaniline-based optical glucose

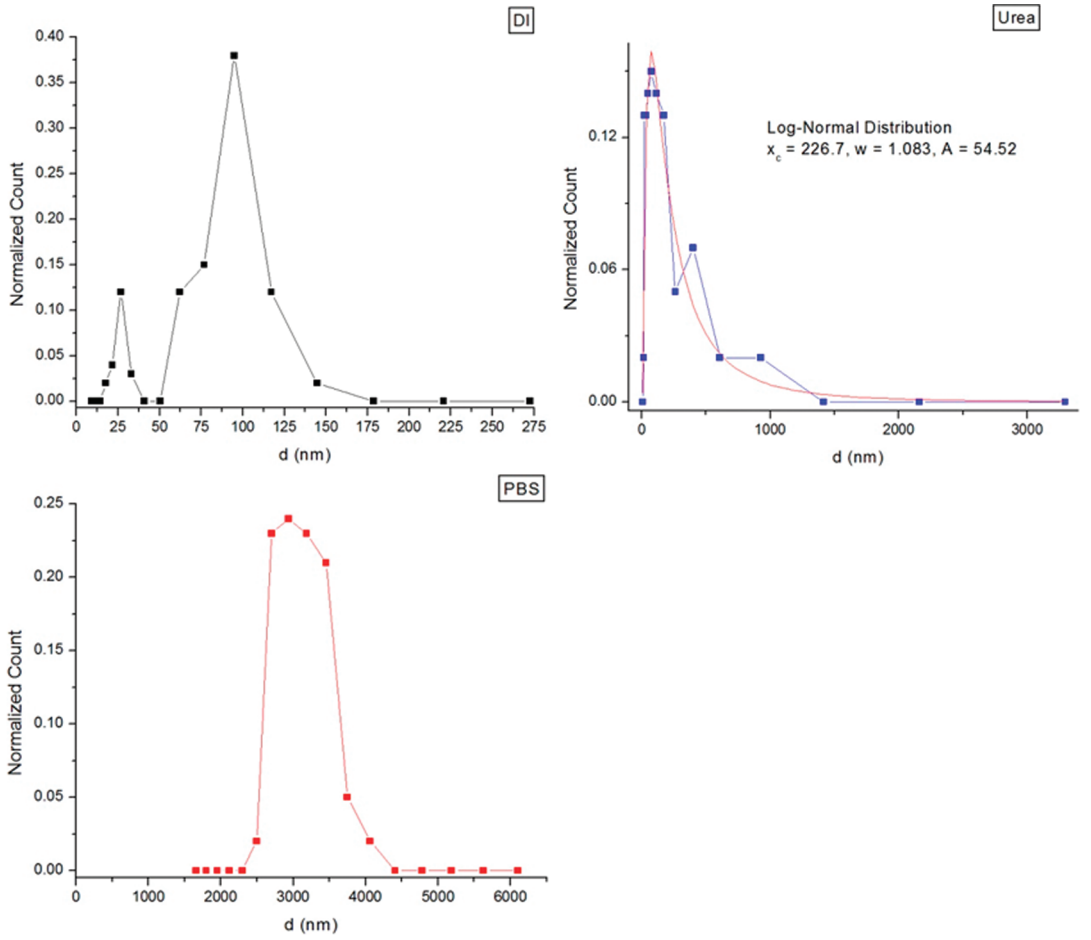

Figure 6. (DI) Half-concentration EB in DI water. The chains are mostly in the extended conformation. (Urea) Particles in 40 mM urea showing a log-normal distribution characteristic of particle aggregation. (PBS) Fully agglomerated (1.5 μm) particles in PBS.

sensors were often intended for *ex vivo* operation only because the sensing element had to be regenerated manually or discarded after each use. The magnitude of the decrease in absorbance at the peak wavelength was fit to the Michaelis−Menten model for enzymatic reactions (Figure 7). The MM relationship was strong as evinced by the double-reciprocal Lineweaver−Burk plot (Figure 7, inset).

The apparent fitting parameters extracted via nonlinear regression were V_{max} = 0.307 mAU and K_M = 0.284 mg/mL (= 1.56 mM).

Discussion

The loss of solubility by increasing the ionic strength is analogous to the "salting out"[40] of proteins using the Hofmeister effect.[41] The effect of ionic salts on polyaniline in a predominately poor solvent environment, such as the systems considered here involving 1:9 NMP:DI, should be contrasted with the case of an unadulterated good solvent. It has been shown that lithium chloride, when added to EB suspended in pure NMP, induces an extended chain conformation. This is due to the reduced interchain hydrogen bonding between the amine and imine groups on neighboring chains as ions displace H-bonds[42] and the chains become increasingly well solvated, which also supports the expanded coil conformation.[44] Additionally, because of pseudodoping, the Li^+ ions cause the chains to become polyionic and therefore polar and soluble. At low ionic strengths, the newly created electrostatic repulsion of charges on the polymer backbone causes it to straighten even further.[43] The overall effect is to greatly reduce the tendency of polyaniline to aggregate[44] and form insoluble particles[20] as confirmed by gel chromatography[45] and scanning electron microscopy.[46] However, at higher[47] (> ~0.15 M) ionic strengths, screening[38] by negative counterions reduces the effect of the positive charges and permits the entropically favored hydrophobic collapse under poor solvent conditions. In this 90% aqueous environment, the critical salt concentration is expected to be much lower because of the large driving force to minimize exposure of the polymer to the majority solvent.

To understand the exciton peak red shift and line-width broadening, it is instructive to consider the closely related conjugated polymer, poly[2-methoxy-5-(2′-ethylhexyloxy)-1,4-phenylenevinylene] (MEH-PPV). In this structure, kinks and ring rotations create conjugation breaks along the chain, giving rise to what can be thought of as separate, but interacting, chromophores.[48] In polyaniline, the situation is even more pronounced because PANI has only a single nitrogen atom between rings instead of an ethylene group. Thus, the steric repulsion between hydrogen atoms on adjacent rings forces even larger torsion angles out of the plane in the ground state.[49] Thus, the chain can be thought of as an ensemble of separate absorbers, with a large distribution of peak wavelengths due to a wide range of conformational disorder. A larger line width is indicative of a wider range of conformations. "Forced planarization"[50] is a likely mechanism for this bathochromic shift that accompanies a conformation change away from a extended strand. In isolated PANI chains the coiling and aggregation of PANI prevents the usual dihedral bending, leading to a larger overlap of the intrachain π-system.[51] Although interchain π-stacking,[52] and its associated electron delocalization, is sometimes invoked for other polymers to explain a reduced bandgap after aggregation, stacking generally leads to the appearance of

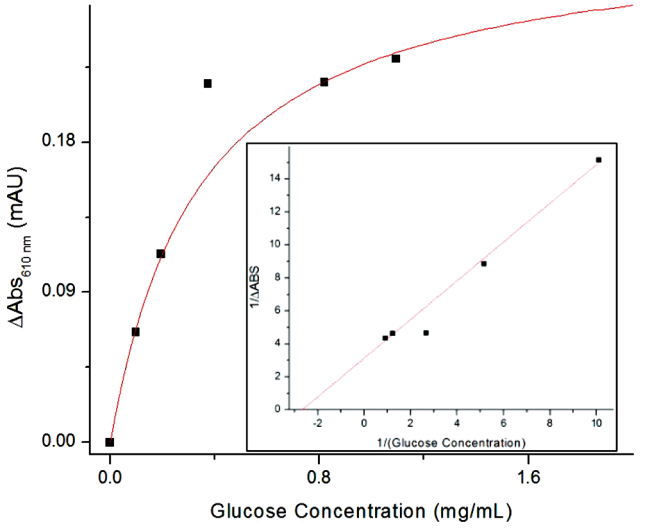

Figure 7. Absorbance change for added amounts of glucose with Michaelis−Menten fit. Extracted apparent constants are V_{max} = 0.307 mAU, K_M = 0.284 mg/mL. The inset shows the corresponding Lineweaver−Burk plot.

a new absorption band, rather than simply the red-shifting of the existing peak, as observed here. The bathochromic shifts that occur after the polymer collapse can also be caused by the additional ions present to screen the charge separation inherent in the exciton, which involves an electron-density transfer from amine to imine sites. Additionally, since the positive ions coordinate with the imine sites, the electron density withdrawn tends to stabilize this process.[20] The change in peak width is likely accounted for by the polydispered nature of the particles. In contrast, the oligomers in THF could not form large particles, so the red shift is less pronounced and occurred at a much higher ionic strength. When some supermolecules did form, it had the opposite effect of tending to equalize the exciton energies among the ensemble, leading to a large decrease in peak width.

In PBS, the preferred environment for enzymes, GOx (isoelectric point 4.2) will carry a negative charge.[53] Thus, it, along with the other negatively charged counterions, is held interstitially by electrostatic interactions with the polymer chains. Once interchain cross-linking causes the polymer to gel, the enzyme remains trapped inside. Because of their small size, Na^+ ions are likely the most important to the pseudodoping process. Indeed, a polaron absorption[54] at 440 nm, indicating that the chain is polyionic, appears when NaCl alone is used in place of PBS. Similarly, Cl^-, as the primary counterion, probably contributes the most to screening. The divalent hydrogen phosphate anions (HPO_4^{2-}), while too large in size and too small in concentration to contribute greatly to screening, can still have a significant effect as ionic "bridges" between chains.[55] However, it is also well established that, based on entropy arguments, multivalent counterions are more likely to coordinate to the chain's backbone compared with monovalent species.[56] In this way too, GOx, as a multivalent anion, can be thought of as an important coordinating and bridging group. This helps explain the larger final size of the aggregated nanoparticles with entrapped GOx compared to those without enzyme.

From the dynamic light scattering data, we see representation from four polymer conformation states. The most extended chains, which are still likely to be loosely coiled to some degree, exist only in pure NMP and the DI water before the addition of precipitating ions. The DI water has a population of collapsed, but separate, coils. When urea is added, there is partial aggregation of these particles, which becomes total agglomeration into microscale particles when PBS is used.

Conclusions

We have demonstrated a novel method for fabricating polyaniline nanoparticles and microparticles with concomitant enzyme entrapment suitable for biosensor fabrication. In the case of glucose oxidase, we have shown that polyaniline can act as both the host polymer and redox indicator. Spectroscopic, light scattering, and SEM evidence was brought to illuminate the abrupt solubility phase transition that occurs when ionic salts disrupt the hydrogen bonding dynamics of the organic−aqueous binary solution. The final morphology and optical properties are sensitive to the relative amounts of polymer, solvent, cosolvent, ions, and enzyme. In this case, the initial polymer concentration was much more dilute than in previous studies, leading to nano- and microscale particles instead of gelled thin films. In addition to biosensing, there are several potential applications for this approach. Since the dynamics of protein folding and aggregation have large implications for human health,[57] the hydrophobic collapse of synthetic homopolymers with easily observed optical features, such as PANI, can serve as model systems for native protein folding[58] as well as potentially pathogenic amyloid agglomeration. Biocompatible nanoparticles that undergo conformation changes depending on their environment may also be used as "smart materials" for controlled *in vivo* drug release.

Acknowledgment. The authors express their appreciation to Dr. Nan-Rong Chiou and Dr. Yong Min for their insight and invaluable suggestions. Additional thanks to Dr. Yun Wu for operating the dynamic light scattering system. This material is based upon work supported in part by the National Science Foundation under IGERT Grant 0221678 and NSEC Grant EEC-0425626 as well as an Ohio State University Institute for Materials Research facilities grant.

References and Notes

(1) Gerard, M.; Chaubey, A.; Malhotra, B. D. *Biosens. Bioelectron.* **2002**, *17*, 345.
(2) Chen, Q.; Kenausis, G. L.; Heller, A. *J. Am. Chem. Soc.* **1998**, *120*, 4582.
(3) Gupta, R.; Chaudhury, N. K. *Biosens. Bioelectron.* **2007**, *22*, 2387.
(4) Campas, M.; Marty, J. L. Encapsulation of Enzymes Using Polymers and Sol-Gel Techniques. *Methods in Biotechnology: Immobilization of Enzymes and Cells*, 2nd ed.; Humana Press: Totowa, NJ, 2006.
(5) (a) Cosnier, S. *Appl. Biochem. Biotechnol.* **2000**, *89*, 127. (b) Trojanowicz, M.; Krawczyk, T. K. *Microchim. Acta* **1995**, *121*, 167.
(6) Parente, A. H.; Marques, E. T. A.; Azevedo, W. M.; Diniz, F. B.; Melo, E. H. M.; Lima Filho, J. L. *Appl. Biochem. Biotechnol.* **1992**, *37*, 267.
(7) (a) Li, Z. F.; Kang, E. T.; Neoh, K. G.; Tan, K. L. *Biomaterials* **1998**, *19*, 45. (b) Chen, Y.; Kang, E. T.; Neoh, K. G.; Tan, K. L. *Eur. Polym. J.* **2000**, *36*, 2095.
(8) Ramanathan, K.; Pandey, S. S.; Kumar, R.; Gulati, A.; Murthy, A. S. N.; Malhotra, B. D. *J. Appl. Polym. Sci.* **2000**, *78*, 662.
(9) Xua, Q.; Zhua, J. J.; Hu, X. Y. *Anal. Chim. Acta* **2007**, *597*, 151.
(10) Horn, D.; Rieger, J. *Angew. Chem., Int. Ed.* **2001**, *40*, 4330.
(11) (a) Foster, E. J.; Berda, E. B.; Meijer, E. W. *J. Am. Chem. Soc.* **2009**, *131*, 6964. (b) Seo, M.; Beck, B. J.; Paulusse, J. M. J.; Hawker, C. J.; Kim, S. Y. *Macromolecules* **2008**, *41*, 6413.
(12) Kamalesh, S.; Tan, P.; Wang, J.; Lee, T.; Kang, E. T.; Wang, C. H.; Kamalesh, S. *J. Biomed. Mater. Res.* **2000**, *52*, 467.
(13) (a) Angelopoulos, M.; Ray, A.; MacDiarmid, A. G.; Epstein, A. J. *Synth. Met.* **1987**, *21*, 21. (b) Virji, S.; Huang, J.; Kaner, R. B.; Weiller, B. H. *Nano Lett.* **2004**, *4*, 491.
(14) Angelopoulos, M.; Asturias, G. E.; Ermer, S. P.; Ray, A.; Scherr, E. M.; MacDiarmid, A. G.; Akhtar, M.; Kiss, Z.; Epstein, A. J. *Mol. Cryst. Liq. Cryst.* **1988**, *160*, 151.
(15) Saprigin, A.; Kohlman, R. S.; Long, S. M.; Brenneman, K. R.; Epstein, A. J.; Angelopoulos, M.; Liao, Y. H.; Zheng, W.; MacDiarmid, A. G. *Synth. Met.* **1997**, *84*, 767.
(16) (a) Sadik, O. A. *Electroanalysis* **1999**, *11*, 839. (b) Xue, H.; Shen, Z.; Li, C. *Biosens. Bioelectron.* **2005**, *20*, 2330.
(17) Zhao, M.; Wu, X.; Cai, C. *J. Phys. Chem. C* **2009**, *113*, 4987.

(18) Parthasarathy, M.; Pillai, V. K.; Mulla, I. S.; Shabab, M.; Parthasarathy; Khan, M. I. *Biochem. Biophys. Res. Commun.* **2007**, *364*, 86.
(19) Hale, P. D.; Inagaki, T.; Karan, H. I.; Okamoto, Y.; Skotheim, T. A. *J. Am. Chem. Soc.* **1989**, *111*, 3482.
(20) Tang, X. Polyaniline: Elucidation of Intrinsic Properties through Processing. PhD Thesis, University of Pennsylvania, **1991**.
(21) Vikki, T.; Pietilä, L. O.; Österholm, H.; Ahjopalo, L.; Takala, A.; Toivo, A.; Levon, K.; Passiniemi, P.; Ikkala, O. *Macromolecules* **1996**, *29*, 2945.
(22) Zheng, W.; Angelopoulos, M.; Epstein, A. J.; MacDiarmid, A. G. *Macromolecules* **1997**, *30*, 7634.
(23) Pouget, J. P.; Jozefowicz, M. E.; Epstein, A. J.; Tang, X.; MacDiarmid, A. G. *Macromolecules* **1991**, *24*, 779.
(24) Oh, E. J.; Min, Y.; Wiesinger, J. M.; Manohar, S. K.; Scherr, E. M.; Prest, P. J.; MacDiarmid, A. G.; Epstein, A. J. *Synth. Met.* **1993**, *55*−*57*, 977.
(25) Zheng, W.; Angelopoulos, M.; Epstein, A. J.; MacDiarmid, A. G. *Macromolecules* **1997**, *30*, 2953.
(26) Jain, R.; Gregory, R. V. *Synth. Met.* **1995**, *74*, 263.
(27) Murgia, S.; Monduzzi, M.; Ninham, B. W. *Curr. Opin. Colloid Interface Sci.* **2004**, *9*, 102.
(28) Dimitriev, O. P.; Getsko, O. M. *Synth. Met.* **1999**, *104*, 27.
(29) MacDiarmid, A. G.; Epstein, A. J. *Synth. Met.* **1994**, *65*, 103.
(30) Angelopoulos, M.; Dipietro, R.; Zheng, W. G.; MacDiarmid, A. G.; Epstein, A. J. *Synth. Met.* **1997**, *84*, 35.
(31) Surwade, S. P.; Agnihotra, S. R.; Dua, V.; Kolla, H. S.; Zhang, X.; Manohar, S. K. *Synth. Met.* **2009**, *159*, 2153.
(32) Traiphol, R.; Sanguansat, P.; Srikhirin, T.; Kerdcharoen, T.; Osotchan, T. *Macromolecules* **2006**, *39*, 1165.
(33) MacDiarmid, A. G.; Chiang, J. C.; Richter, A. F.; Epstein, A. J. *Synth. Met.* **1987**, *18*, 285.
(34) Beljonne, D.; Pourtois, G.; Silva, C.; Hennebicq, E.; Herz, L. M.; Friend, R. H.; Scholes, G. D.; Setayesh, S.; Müllen, K.; Brédas, J. L. *Proc. Natl. Acad. Sci. U.S.A.* **2002**, *99*, 10982.
(35) Nguyen, T. Q.; Doan, V.; Schwartz, B. J. *J. Chem. Phys.* **1999**, *110*, 4068.
(36) Liu, S.; Ghosh, K.; Muthukumar, M. *J. Chem. Phys.* **2003**, *119*, 1813.
(37) Zheng, W.; Min, Y.; MacDiarmid, A. G.; Angelopoulos, M.; Liao, Y. H.; Epstein, A. J. *Synth. Met.* **1997**, *84*, 63.
(38) Gettinger, C. L.; Heeger, A. J.; Pine, D. J.; Cao, Y. *Synth. Met.* **1995**, *74*, 81.
(39) Lee, S. R.; Sawada, K.; Takao, H.; Ishida, M. *Biosens. Bioelectron.* **2008**, *24*, 650.
(40) Parsegian, V. A. *Nature* **1995**, *378*, 335.
(41) Baldwin, R. L. *Biophys. J.* **1996**, *71*, 2056.
(42) Zheng, W.; Angelopoulos, M.; Epstein, A. J.; MacDiarmid, A. G. *Macromolecules* **1997**, *30*, 2953.
(43) Seery, T. A. P.; Angelopoulous, M.; Levon, K.; Seghal, A. *Synth. Met.* **1997**, *84*, 79.
(44) Angelopoulos, M.; Liao, Y. H.; Furman, B.; Graham, T. *Macromolecules* **1996**, *29*, 3046.
(45) (a) Angelopoulos, M.; Liao, Y. H.; Furman, B.; Graham, T. *SPIE Opt. Photonic Appl. Electroactive Conducting Polym.* **1995**, *2528*, 230. (b) Wang, F. S.; Jing, X. B.; Wang, X. H.; Dong, A. J. *Synth. Met.* **1995**, *69*, 93.
(46) Chao, D.; Chen, J.; Lu, X.; Chen, L.; Zhang, W.; Wei, W. *Synth. Met.* **2005**, *150*, 47.
(47) Degani, Y.; Heller, A. *J. Am. Chem. Soc.* **1989**, *111*, 2357.
(48) Scholes, G. D.; Rumbles, G. *Nat. Mater.* **2005**, *5*, 683.
(49) Ginder, J. M.; Epstein, A. J. *Phys. Rev. Lett.* **1990**, *64*, 1184.
(50) Bunz, U. H. F. *Chem. Rev.* **2000**, *100*, 1605.
(51) Miteva, T.; Miteva, T.; Palmer, L.; Kloppenburg, L.; Neher, D.; Bunz, U. H. F. *Macromolecules* **2000**, *33*, 652.
(52) Bertinelli, F.; Costa-Bizzarri, P.; Della-Casa, C.; Lanzim, M. *Synth. Met.* **2001**, *122*, 267.
(53) Wang, G.; Thai, N. M.; Yau, S. T. *Electrochem. Commun.* **2006**, *8*, 987.
(54) Stafström, S.; Brédas, J. L.; Epstein, A. J.; Woo, H. S.; Tanner, D. B.; Huang, W. S.; MacDiarmid, A. G. *Phys. Rev. Lett.* **1987**, *59*, 1464.
(55) Kundagrami, A.; Muthukumar, M. *J. Chem. Phys.* **2008**, *128*, 244901.
(56) Hinderberger, D.; Jeschke, G.; Spiess, H. W. *Macromolecules* **2002**, *35*, 9698.
(57) Chiti, F.; Dobson, C. M. *Annu. Rev. Biochem.* **2006**, *75*, 333.
(58) Nelson, J. C.; Saven, J. G.; Moore, J. S.; Wolynes, P. G. *Science* **1997**, *277*, 1793.